



## Research article

## The impact of secondary mineral formation on Na-K-geothermometer readings: a case study for the Valley of Geysers hydrothermal system (Kronotsky State Nature Biosphere Reserve, Kamchatka)

Anastasia V. SERGEEVA<sup>1</sup>✉, Alexey V. KIRYUKHIN<sup>1,2</sup>, Olga O. USACHEVA<sup>1</sup>, Tatiana V. RYCHKOVA<sup>1</sup>, Elena V. KARTASHEVA<sup>1</sup>, Mariya A. NAZAROVA<sup>1</sup>, Anna A. KUZMINA<sup>1</sup>

<sup>1</sup> Institute of Volcanology and Seismology FEB RAS, Petropavlovsk-Kamchatsky, Russia

<sup>2</sup> Kronotsky State Nature Biosphere Reserve, Yelizovo, Russia

**How to cite this article:** Sergeeva A.V., Kiryukhin A.V., Usacheva O.O., Rychkova T.V., Kartasheva E.V., Nazarova M.A., Kuzmina A.A. The impact of secondary mineral formation on Na-K-geothermometer readings: a case study for the Valley of Geysers hydrothermal system (Kronotsky State Nature Biosphere Reserve, Kamchatka). *Journal of Mining Institute*. 2023. Vol. 262, p. 526-540. EDN BMBZHP

**Abstract.** The temperature in the Valley of Geysers (Kamchatka) geothermal reservoir calculated using the feldspar Na-K-geothermometer has been steadily increasing over the past 10 years on average from 165 to 235 °C, which is close to the temperature values of a hydrothermal explosion of the steam and water mixture. For the analysis of chemical geothermometers, TOUGHREACT-simulation was used, with the help of which the previously known Na-K feldspar geothermometer was reproduced on a single-element model and new formulas were obtained for three Na-K-geothermometers: zeolite, smectite, and based on volcanic glass. Data of chemical analysis for the period 1968-2018, in which the chloride ion is considered as an inert tracer of geofiltration processes, indicates that after 2007 a significant inflow of infiltration water (its mass fraction is estimated from 5 to 15 %) into the Geyser reservoir. It is assumed that the Na-K increased values of the feldspar geothermometer are not the result of the temperature increase in the Geyser reservoir, but the effect of smectite water dilution.

**Keywords:** TOUGHREACT-simulation; Valley of Geysers; geothermometers; zeolites; montmorillonite; geothermal reservoir; volcanic glass

**Acknowledgments.** The research was financially supported by the RFBR and Science and Technology Research Council of Japan within the RFBR scientific project N 21-55-50003 YaF\_a “Magmatic fracking and fluid flows in volcanic structures” and the IVIS FEB RAS research project N FWEW-2019-0002 “Heat-mass transfer and seismicity in hydrothermal, magmatic and geofluid systems, thermohydrodynamic-geochemical-geomechanical modeling (TOUGH2, TOUGHREACT, C-FRAC), applications to geothermal resource assessment and earthquake prediction”.

Received: 13.04.2022

Accepted: 13.02.2023

Online: 22.06.2023

Published: 28.08.2023

**Introduction.** Temperature and gas phase pressure and saturation define thermohydrodynamic conditions of geofluid reservoirs. These are the main parameters, from which all other heat transfer fluid parameters (enthalpy, viscosity, density of the liquid and gas phases, etc.) can be calculated. Geochemical thermometers are widely used in prospecting, exploration and analysis of geothermal reservoir conditions, which allow estimating the temperature in a productive geothermal reservoir from the chemical composition of a heat transfer fluid without drilling or direct temperature measurements in wells. For example, the formation temperature assessment of the Pyatigorsk mineral water deposit revealed two temperature ranges of their formation: one for the soda composition waters and the other for the waters with the sodium sulfate predominance [1]. We estimated the fluid generation temperatures of mud volcanoes in Azerbaijan using the Na-Li- and Mg-Li-geothermometers designed to estimate temperatures in the range of up to 300-340 °C of water formation layers in sedimentary basins, including oil ones [2]. The formation conditions of the Ulsky thermal spring



located on the Sea of Okhotsk coast (Khabarovsk Krai), revealed using geothermometry, indicate the 1-2 km deep water circulation, at the temperature that does not exceed 80 °C [3]. In Kyrgyzstan, the research of more than two dozen of thermal and cold mineral waters located in the northern and southwestern Tien Shan, using the Na-K-geothermometers revealed that they are formed without any endogenous heat source under the influence of local temperature gradients [4]. Geothermometric research of thermal springs located in the Pamirs and the foothills of the Tien Shan (Tajikistan) showed that the waters were formed at temperatures of up to 240 °C [5, 6]. The Okinsky hydrothermal system, located in the Eastern Sayan and associated with the basaltic volcanism manifestation was studied using a number of geothermometers [7]. The use of geothermometers during the study of nitrogen thermal waters in Jiangxi Province (China) revealed the problem of the temperature estimation accuracy, associated with mixing, and showed that the Na-K-geothermometer is less sensitive to the impact of ground and meteoric waters than the SiO<sub>2</sub>-geothermometer [8]. Geothermometric research was carried out to define the conditions for the formation of the Tavatum nitrogen thermal waters located on the Sea of Okhotsk coast of the Magadan Region [9]. In general, geothermometry along with isotopy is used to define the conditions for the waters of various genesis formation, while there is a problem of their correct use, which is taken into account by the researchers.

The method of chemical geothermometers is based on the use of the dependence between the chemical equilibrium constants between the fluid and the host rocks [10]. The sodium-potassium geothermometer is most widely used for geothermal reservoirs with the temperature that exceeds

150 °C  $t(\text{Na-K}) = \frac{855.6}{\lg \left[ \frac{C(\text{Na}^+)}{C(\text{K}^+)} \right] + 0.8573} - 273.15$  [11], it is based on the feldspar equilibria

and is fairly well tested in drilled geothermal deposits. The following type of the geothermometer

is also applicable  $t(\text{Na-K}) = \frac{1217}{\lg \left[ \frac{C(\text{Na}^+)}{C(\text{K}^+)} \right] + 1.438} - 273.15$  [12].

Checking the condition  $T > 150$  °C, if drilling wells for direct temperature measurement is obviously impossible, is a non-trivial and urgent task in the Valley of Geysers of the Kronotsky State Nature Biosphere Reserve, where drilling is prohibited by current legislation. This problem solution is important for the safety of the tourism infrastructure in the Valley of Geysers, which is annually visited by about 6,000 people with a tendency of increasing the attendance. The temperature calculated using the feldspar Na-K-geothermometer has been steadily increasing over the past 10 years, from 165 to 235 °C [13]. The temperature increase in a two-phase geothermal reservoir means simultaneous pressure increase from 7 to ~31 bar, respectively, which can lead to destruction of the upper confining layer, up to 10-20 m thick, and hydrothermal explosion in the epicenter of the Geyser reservoir, similar to the 2007 catastrophic collapse and the 2014 mudflow, which were caused by hydrothermal activity [14, 15].

Two approaches are used in the geochemical assessment of the temperature in geothermal reservoirs. According to the first, the temperature is determined by the ratio of elements in solution. The ratio of sodium and potassium concentrations, the silica content in the solution, the Na-K-Ca ratio, and a number of other functions correlating the elements concentrations with the temperature are often used, with the preference given to the most easy-to-use mathematical expressions. The Na-K-geothermometer, developed for water equilibria with feldspars is very popular. It could easily be used as it allows us to get rid of dilution effects, and due to the wide occurrence of feldspars, the geothermometer can be used in a wide range of hydrogeological conditions. The constraints in the geothermometer use are related to the equilibrium between water and the rock-forming minerals. For example,



the classical expressions for the Na-K-geothermometers are defined for the feldspars and thermal waters equilibrium [10], and when the host rocks mineral composition changes, as happens in geothermal reservoirs, the temperature estimation may become incorrect. The second approach for temperature assessment is based on the selection of the mineral composition, which is in equilibrium with the chemical composition of water. For example, the program iGeoT helped to minimize saturation indices for this approach [16].

Over the period of 1969-2003, the use of Na-K-geothermometer in the Valley of Geysers indicated slow (from 0.3 to 0.9 °C/year) temperature decrease in the reservoir, within the range of 165-185 °C. After the giant landslide of June 3, 2007, the slow downward trend was replaced by rapid (from 4.2 to 5 °C/year) temperature increase, and the temperature range shifted towards higher temperatures (180-230 °C) (Fig.1). The temperature increase in the Geyser reservoir was possibly caused by two independent reasons. The first possible reason relates to Kikhpinych Volcano magmatic activity. This hypothesis is supported by the volcano activity, which was considered in detail in [17]. The activity of Kikhpinych seems to be an unlikely reason for the increase in geochemical temperature, since volcanic gases should have caused a decrease in pH and an increase in the Cl content in the waters, which was not observed. The second probable reason is due to incorrect use of the feldspar Na-K geochemical thermometer in conditions of existence of other mineral phases, capable of ion exchange, including those with sodium and potassium.

The active mineral-forming processes and the host rocks processing resulted in formation of the whole range of secondary minerals, among which the most interesting for us are those that are capable of ion exchange with sodium and potassium. At this time it is well known that, depending on pH and solution composition, in the areas of high-temperature discharges zeolite minerals, such as mordenite, stilbite, heulandite, and clinoptilolite [18, 19], or the layered silicates of the smectite group, most often montmorillonite [20, 21] and a number of other deposits [22, 23] are formed. Zeolites are formed in alkaline media, while montmorillonite is formed under slightly acidic and nearly neutral conditions [24]. Along with montmorillonite, kaolinite is also formed in thermal fields, but due to its low ability for proper ion exchange, it is not considered in this work; moreover, it is favoured by acidic and slightly acidic media, which practically do not meet the conditions of geyser discharges [19, 20].

Zeolites are tektosilicates which structure contains channels and cavities sufficient for ion exchange with sodium and potassium cations existing in solution. In layered silicates, cations located in the interlayer space are also easily exchanged for cations of the contacting solution. At that, in nature, usually both zeolites and smectite minerals are finely dispersed, they easily disperse and form

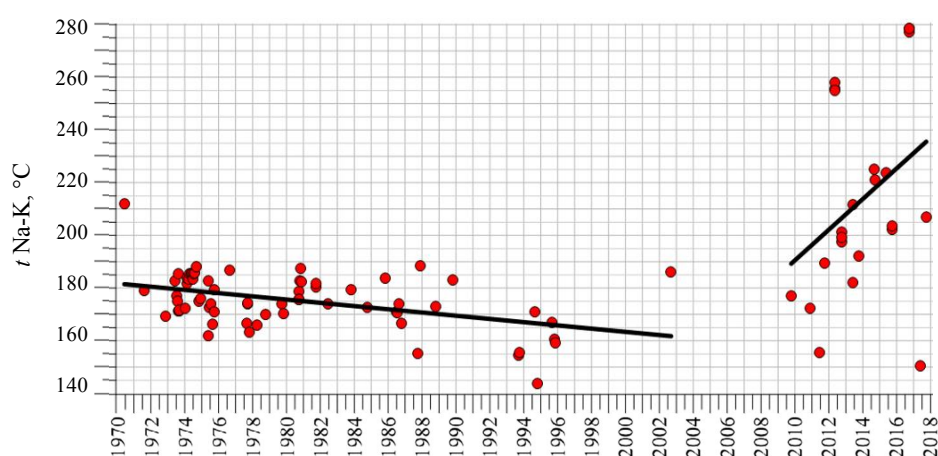


Fig.1. Calculated temperature variants obtained using the feldspar Na-K-geothermometer [11, 25] for Velikan Geyser (the Valley of Geysers, Kamchatka) in 1969-2016 [14]



a suspension; therefore, equilibrium with solutions in terms of sodium and potassium cations for zeolite and montmorillonite minerals is achieved relatively quickly.

The high rate of ion exchange in clinoptilolite was considered in some works [26, 27] describing the kinetic parameters and factors determining the mechanism and rate of ion exchange processes [28, 29]. Natural zeolites seem to be the optimal material for a number of practical applications, for example, for production of catalysts and sorbents [30]. For example, the modification of zeolitized tuffs containing mordenite and clinoptilolite made it possible to obtain catalysts for the light oil fractions transformation [31].

Wastewater radioactive decontamination and other complete treatment at mining and processing enterprises and nuclear industries is possible using zeolite sorbents [32, 33]. Ion exchange processes have an impact on heavy metals in soils accumulation [34, 35], they should also be taken into account in the disposal of nuclear waste [36, 37].

Ion exchange characteristics of montmorillonite are related to its ability to swell, which is taken into account when developing oil reservoirs [38]. The relevance of a comprehensive study is confirmed by the work on the analytical control of the content of petroleum products [39-41]. No less promising cation exchanger with fast kinetics is montmorillonite [42, 43], a layered silicate, the ion exchange properties of which are due to heterovalent substitutions in metal-oxygen networks [44, 45] and the spatial organization of clay particles [46]. Montmorillonite is actively formed in thermal fields of modern hydrothermal systems [20], where, under complex dynamic conditions, it exchanges with contacting solutions [10, 47]. Summing up, we should note that while interacting with finely dispersed zeolites and montmorillonite the cations equilibrium time is from several tens of minutes to a day, and in case of feldspars this time ranges from hundreds to tens of thousands of years or more [10]. Therefore, it can be assumed that waters in contact with mudflow deposits or secondary minerals in the Geyser reservoir or in the zones of surface water infiltration relatively quickly take on the sodium and potassium ratios that are characteristic of montmorillonite or zeolites [10, 18, 48].

Volcanic glass existing in the host rocks composition of the Geyser reservoir, is characterized by wide variations in composition, it dissolves relatively easily, especially in alkaline media, it is metastable to crystalline phases transition, and therefore can have significant effect on composition of contacting with it waters [18].

Catastrophic processes (the 2007 catastrophic collapse and the 2014 mudflow) in the Valley of Geysers led to partial destruction of the upper confining layer, infiltration windows formation and the geysers channels flooding, which resulted in significant inflow of infiltration surface water into the productive Geyser reservoir [49] that also should be considered when choosing geothermometers.

**Hydrogeological stratification and mineralogical composition of the Geyser productive reservoir.** The area is characterized by the accumulative volcanic type of relief, the formation of which is mainly associated with the volcanogenic deposits accumulation. The oldest Lower-Middle Pleistocene effusive-pyroclastic strata are exposed mainly in depressions and calderas sides, while young Upper Pleistocene and Holocene ones form vast plateaus, as well as stratovolcanoes, cinder cones, and extrusive domes. The area of the Geysernaya River is composed of the volcanic-sedimentary stratum, which is the complex interchange of different layers: tuff breccias, agglomerate tuffs, psammite tuffs and aleuopelitic tuffs. Pressed clustered pumices are also widespread. The volcanogenic-sedimentary stratum is intruded by different age andesites and andesite-dacites extrusions, with which short lava flows are associated [50, 51].

The Quaternary 1 km or more thick strata of relatively loose pyroclastics and their erosion products, fill the depressions and have fairly good reservoir properties, which creates the conditions for the thermal waters reservoir formation in these deposits [52]. The bulk of hydrothermal manifestations emerge from the original outcrops of poorly lithified pumiceous psephytic and agglomerate tuffs and dacites of the geyser and estuarine formations. One of the important geological and structural factors in the formation and activity of the high-temperature hydrothermal system of the Valley of





Geysers is low psephytic tuffs permeability of the Geyser and estuarine formations, which prevents the intensive intrusion of cold surface waters. The upper part of the section of the Geyser and estuarine formations is composed, among other things, of fine-grained varieties of tuffs, the pore permeability coefficients of which, as a rule, are two orders of magnitude lower than those of psephytic tuffs. They serve as the upper confining layer and contribute to the better waterproofing of water-bearing horizons [50].

The geyser productive reservoir is formed as a result of successive series of pipes of hydrothermal explosions followed by chemical dissolution/suffusion of the central geyser channels and self-sealing by secondary hydrothermal minerals of the peripheral parts and the roof (upper waterproof rock) [14], the inflow of the deep thermal fluid is confined to channels/dykes. The upper waterproof rock is the product of hydrothermal processing of the original rocks.

It was shown in [13] that both hydrothermally altered and unaltered aleuropelitic vitroclastic and psammitic-psephytic pumice rocks with inclusions of litho- and crystal clasts are distributed in the Geyserny formation (grn), which was exposed by the 2007 collapse, while hydrothermal transformations are subject to first of all, volcanic glass and pumice clasts, the share of which in the initial mineralogical composition is significant.

In the central part of the Uzon Caldera, on the left bank of the Shumnaya River (Mt. Belaya), there is an extrusion composed of pumice stones ( $Q_3$ ), practically unaffected by hydrothermal transformations. Its composition, expressed in terms of feldspar and quartz content, is as follows: 44 wt.%  $NaAlSi_3O_8$ , 29 %  $SiO_2$ , 15 %  $KAlSi_3O_8$ , 12 %  $CaAlSi_2O_8$ . The mineral composition, according to X-ray phase analysis, corresponds to the elemental composition, namely, the feldspars and volcanic glass predominance.

**Methods.** *Source data for TOUGHREACT-simulation, assembly of the simulation.* The geyserites mineral composition was revealed using loggers for the geysers temperature and eruptive cycle monitoring. A logger is a special small metal cylinder of about 10 cm long and about 1 cm in diameter that should be immersed in the researched medium for data recording over the period of several months. The six months of logger operation, allow us to obtain actual data on the geyserites mineral composition resulted from a thin layer of geyserite deposits, covering the logger, at that *the unique geyserite structures do not suffer*, and the current data on the mineral composition of geyserites are at the disposal of researchers.

The mineral composition was studied using X-ray diffractometry. The X-ray diffractograms were recorded using the X-ray diffractometer MaxXRD 7000 (Shimadzu) in the range of  $6-65^\circ 2\theta$  with the  $0.05-0.1^\circ 2\theta$  step, scanning speed 1-2 deg/min, which is equivalent to exposure at a point of 3-6 s. The semi-quantitative sediments composition was analyzed by means of the X-ray fluorometry method, using the S4 Pioneer spectrometer (BrukerAXS). All the studies were made in the Analytical Center of the IVS FEB RAS.

Previously, we revealed that geyserite sinters have predominantly quartz-opal-ceolitic composition with different ratios of mineral components [19]. The diffractograms of logger deposits show an intense halo, which corresponds to amorphous phases with a small coherent scattering region (Fig.2). The study of the composition of the logger sediments for the period 2018-2021 showed that the 2018 well-crystallised sediments gradually become more amorphous, and by 2021 the degree of crystallinity had become very low (Fig.2). Simultaneously with the decrease in crystallinity, the composition of the sediments also changes: amorphous hydrated silica becomes the dominant phase rather than zeolites. This can be caused by a decrease in pH, a decrease in the concentration of silica and aluminum in thermal solutions, and a decrease in temperature. It is known that alkaline environment is favourable for crystallization of zeolites, as pH increase causes their crystallization rate increases as well. In contrast, no temperature decrease has been observed; geysers discharged and keep discharging during eruptions at about  $100^\circ C$ .



The diffractograms show diffused reflexes, which may belong to zeolites such as mordenite, haylandite, clinoptilolite and, possibly, stilbite. These zeolites have similar diffractograms, and if the amorphous component predominates, the broadened reflexes overlap each other and hinder precise identification.

The authors have designed one-element model in the TOUGHREACT-EOS2 software package [53, 54], its scheme is shown in Fig. 3. Initial conditions are as follows: pressure 60 bar, temperature 210 °C, partial pressure of CO<sub>2</sub> is set to zero. The material properties of the model are defined as follows: density 2700 kg/m<sup>3</sup>; porosity 0.1; permeability 10<sup>-12</sup> m<sup>2</sup>; thermal conductivity 2 W/(m·°C); heat capacity – 850 J/(kg·°C). Specific water discharge corresponds to the productive Geyser reservoir, water composition corresponds to that typical for Geyser Velikan (Giant) (Table 1). Host rock minerals: glass\*<sup>3</sup> Na<sub>0.97</sub>Ca<sub>0.016</sub>K<sub>0.005</sub>Mg<sub>0.0015</sub>Si<sub>2.99</sub>Al<sub>1.01</sub>O<sub>8</sub>; smectite-Na Na<sub>x</sub>[Al, Mg, Fe]<sub>2</sub>[Si<sub>4</sub>O<sub>10</sub>](OH)<sub>2</sub>; smectite-K K<sub>x</sub>[Al, Mg, Fe]<sub>2</sub>[Si<sub>4</sub>O<sub>10</sub>](OH)<sub>2</sub>; smectite-Ca Ca<sub>x</sub>[Al, Mg, Fe]<sub>2</sub>[Si<sub>4</sub>O<sub>10</sub>](OH)<sub>2</sub>; albite NaAlSi<sub>3</sub>O<sub>8</sub>; microcline KAlSi<sub>3</sub>O<sub>8</sub>; anorthite CaAl<sub>2</sub>Si<sub>2</sub>O<sub>8</sub>; opal SiO<sub>2</sub>·nH<sub>2</sub>O; mordenite [Na<sub>2</sub>, Ca, K<sub>2</sub>]<sub>4</sub>[Al<sub>8</sub>Si<sub>40</sub>]O<sub>96</sub>·28H<sub>2</sub>O; clinoptilolite Ca<sub>3</sub>[Si<sub>30</sub>Al<sub>6</sub>]O<sub>72</sub>·20H<sub>2</sub>O.

The model is designed as a cube with side of 100 m (Fig.3) and flow-through circulation with constant flow rate of 5.8 kg/s. The flow-through circulation is defined by water extraction from a modeled borehole with simultaneous injection of constant flow rate with given enthalpy into the model element (inflow of deep heat transfer fluid or infiltration water). The simulation time is equal to 1000 years.

**The results of the TOUGHREACT-simulation.** Derivation of Na-K-geothermometer equations for different minerals. When processing the results of TOUGHREACT-simulation, we assume that the ion product or the ion exchange constant corresponds to the Arrhenius plot on temperature  $T: K(T) = A_{\text{exp}}(-\Delta G/RT)$ , where  $A$

is a multiplier almost independent of temperature;  $\Delta G$  is the change in Gibbs energy during the reversible process;  $R$  is the universal gas constant. During the simulation at different values of enthalpy (inflow of deep heat transfer fluid or infiltration water), we obtained the composition of the solution in equilibrium with a given set of minerals at the temperature range 25-250 °C. The simulation data

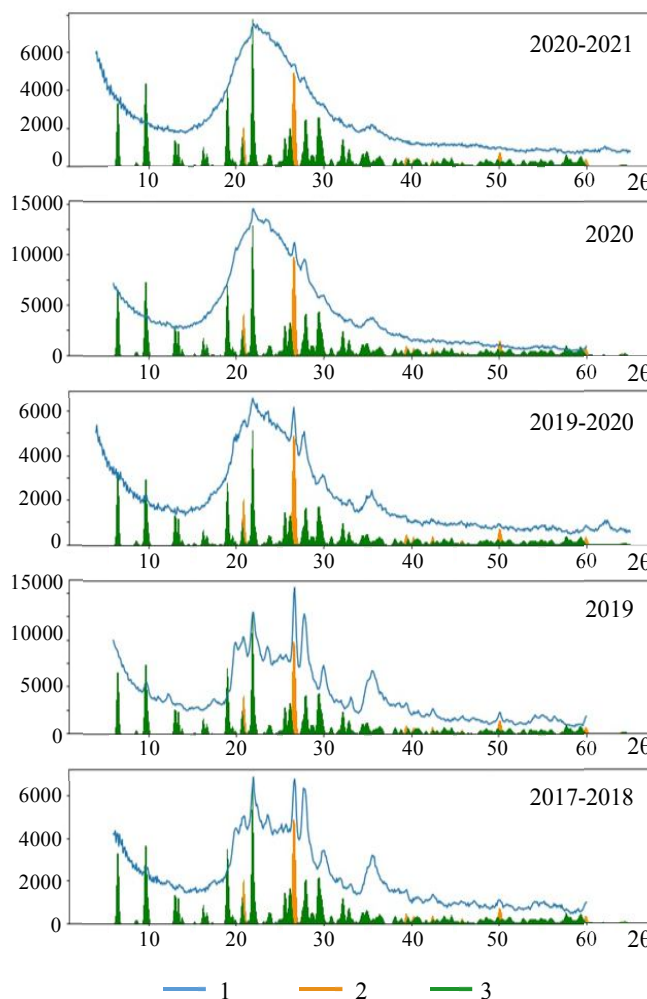


Fig.2. Deposits of Giant Geyser obtained in 2017-2021  
1 – mineral deposits; 2 – quartz; 3 – zeolite

Table 1

**Water composition used in the simulation, which corresponds to a composition close to that of Geyser Giant (pH = 8)**

Component	Concentration	
	mol/kg H <sub>2</sub> O	mg/l
NH <sub>4</sub> <sup>+</sup>	5.6·10 <sup>-5</sup>	1
Na <sup>+</sup>	2.64·10 <sup>-2</sup>	605
K <sup>+</sup>	1.2·10 <sup>-3</sup>	47
Ca <sup>2+</sup>	5.5·10 <sup>-4</sup>	22
SiO <sub>2</sub>	5.0·10 <sup>-3</sup>	300
AlO <sub>2</sub> <sup>-</sup>	1.0·10 <sup>-7</sup>	5.9·10 <sup>-3</sup>
Cl <sup>-</sup>	2.46·10 <sup>-2</sup>	872
SO <sub>4</sub> <sup>2-</sup>	1.68·10 <sup>-3</sup>	161
HCO <sub>3</sub> <sup>-</sup>	1.44·10 <sup>-3</sup>	88

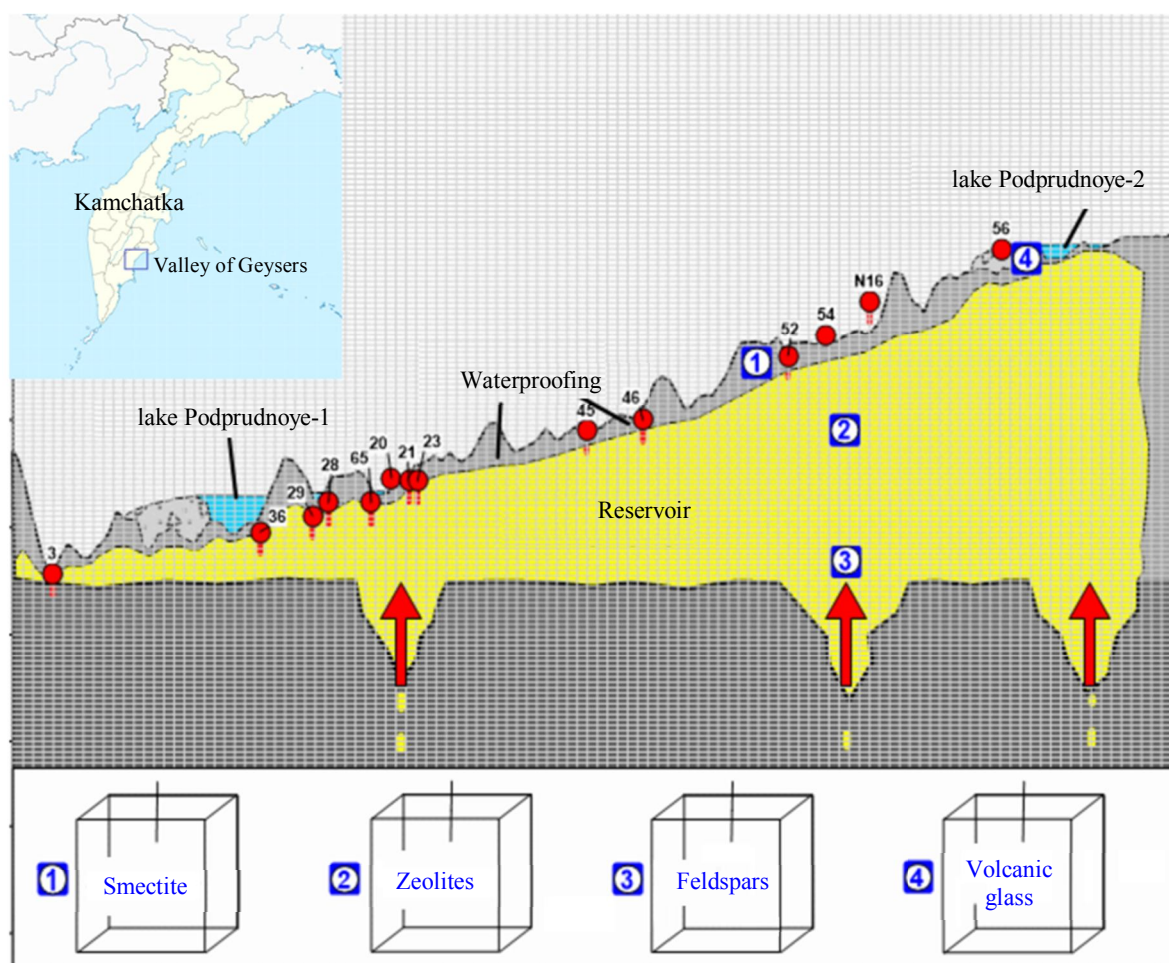


Fig.3. One-element model simulating a part of the Geyser reservoir in zones with different mineral compositions [55]

1 – K-montmorillonite + Na-montmorillonite + Ca-montmorillonite; 2 – mordenite + clinoptilolite (clinopt/10);  
3 – feldspar + high albite + low albite; 4 – volcanic glass (glass3); the inset shows location of the Valley of Geysers in Kamchatka

of the water equilibrium composition were converted into the coordinates  $1000/T$  and  $\lg(C_i/C_j)$ , where  $C_i$  and  $C_j$  are concentrations of the corresponding solution components in mass or molar units (g/l, mg/l, ppm, mol/l, etc.).

The linearized sections of the obtained plots were described by an equation  $y = A + Bx$ , where  $y = \lg(C_i/C_j)$ ;  $x = 1000/(t + 273.15)$ , from which the following geothermometer equation was derived

$$t = \frac{1000B}{\lg \left[ \frac{C(\text{Na}^+)}{C(\text{K}^+)} \right] - A} - 273.15.$$

During the simulations the authors got solution composition data where concentrations are expressed in mol/l. In order to convert to mass concentrations, we need to multiply by the molar mass, and to convert the  $C_i/C_j$  ratio from molar to mass units, we need to multiply this value by the  $Mr_i/Mr_j$  factor, where  $Mr_i$  and  $Mr_j$  are the molar masses of components  $i$  and  $j$ . The conversion factor for the ratio of sodium and potassium concentrations from molar units to mass units is 23/39. For convenience, the units of sodium and potassium concentrations are indicated next to each equation and on the corresponding graphs later in the text.

Table 2 shows the results of water – rock interaction simulation for various epigenetic minerals, with constant initial water composition and constant flow rate. The table shows the values of coefficients  $A$  and  $B$  and indicates the temperature ranges of linear or close to linear sections.



Table 2

Equation coefficients  $t = \frac{1000B}{\lg \left[ \frac{C(\text{Na}^+)}{C(\text{K}^+)} \right]^{-A}} - 273.15$  for various minerals

Mineral assemblage	Temperature range, °C	Coefficients	
		A (for ppm)	B
Albite, anorthite, microcline	25-250	-1.683	1.239
Glass	25-125	0.961	0.037
	125-250	1.034	0.0085
Montmorillonite	25-125	-1.267	0.612
Zeolites (mordenite, heulandite, clinoptilolite)	25-125	1.151	-0.012
	125-250	1.949	-0.349

*K-feldspar + low albite + water system (T4\_REACT\_Feldspar).* We took K-feldspar and low albite in equal volumetric fractions as initial phases, with the addition of the high-temperature albite modification that does not change the pattern. The simulation time was equal to 1000 years and a water-rock chemical equilibrium was assumed at each simulation step.

The feldspar geothermometer derived during the simulation is close to the classic Fournier equation [12, 56], and provides consistent results. The range in which the Na/K ratio varies is quite large, it is about 2.5 to 300, and this fact allows us to determine the temperature quite well using the cation content. High ratios are typical for low temperatures and vice versa, therefore application of feldspar geothermometer for cases when sodium is absorbed and  $C(\text{Na})/C(\text{K})$  ratio decreases, leads to apparent warming of geothermal reservoir (Fig.4) [57].

The equation of the feldspar geothermometer is as follows:

$$t = \frac{1239}{\lg \left[ \frac{C(\text{Na}^+)}{C(\text{K}^+)} \right] + 1.683} - 273.15 \text{ ppm.}$$

*Glass (glass3) + water system (TR\_T\_glass3\_#9).* Only volcanic glass3 was taken as initial phases. The simulation time was equal to 1000 years; at each simulation step local chemical water-rock equilibrium was assumed.

During the simulation we detected a glass dissolution, while the logarithm of the  $C(\text{Na})/C(\text{K})$  ratio varied insignificantly between 1.28 and 1.32 (mol/l) (Fig.5), so the actual use of the geothermometer based on volcanic glass is complicated. Within the range of 125-250 °C, the geothermometer equation is as follows:

$$t = \frac{8.5}{\lg \left[ \frac{C(\text{Na}^+)}{C(\text{K}^+)} \right] - 1.034} - 273.15 \text{ ppm;}$$

within the range of 25-125 °C the geothermometer equation based on the volcanic glass:

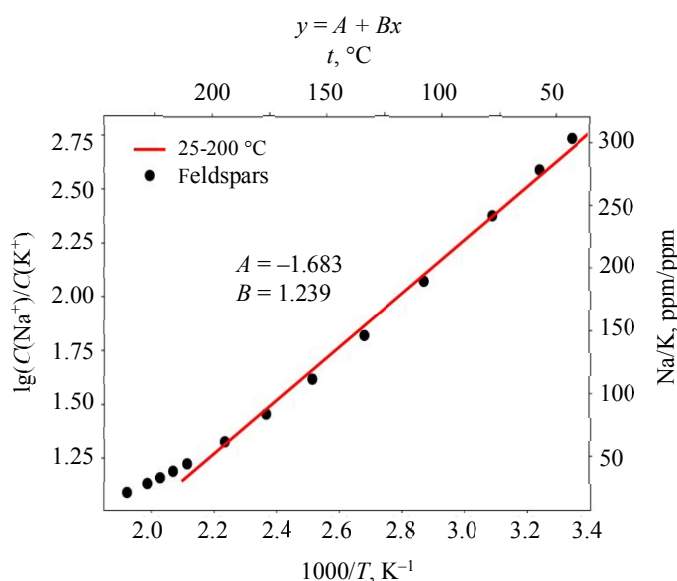


Fig.4. Arrhenius plot for the sodium-potassium ratio (ppm) in the case of equilibrium between thermal waters and feldspars



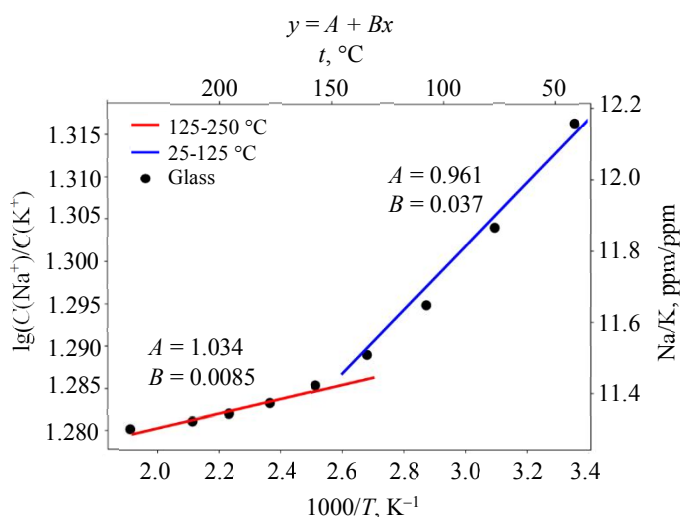


Fig.5. Two linear sections in Arrhenius coordinates corresponding to the temperature dependence of the ratio of sodium and potassium concentrations for glass

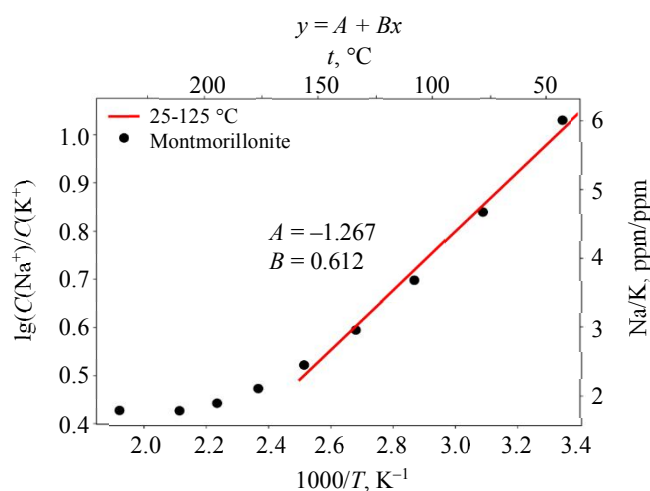


Fig.6. Linear section of sodium-potassium concentration ratio for equilibrium between montmorillonite and thermal waters

versa. The graph (Fig.6) shows a linear section in the temperature range of 25-125 °C. The small range of ratio variation and low relative sodium content does not allow using feldspar Na-K-geothermometer for temperature estimation in case of smectite control of sodium/potassium ratio. In the 25-150 °C range the geothermometer equation:

$$t = \frac{612}{\lg \left[ \frac{C(\text{Na}^+)}{C(\text{K}^+)} \right] + 1.267} - 273.15 \text{ (for ppm).}$$

At thermal fields of Kamchatka, montmorillonite is predominantly sodium-calcium; waters that are in equilibrium with it are characterized by a low  $C(\text{Na})/C(\text{K})$  ratio, so the use of feldspar geothermometer leads to apparently significant warming of the geothermal reservoir. Meanwhile, in mud-and-water pots of modern thermal fields in Kamchatka with weakly acidic and near-neutral waters, if montmorillonite is a dominant mineral, we observe smectite control of sodium and potassium concentration ratio, at which they lie within the calculated limits of 1.5-6 (for ppm) [58].

$$t = \frac{37}{\lg \left[ \frac{C(\text{Na}^+)}{C(\text{K}^+)} \right] - 0.961} - 273.15 \text{ ppm.}$$

Glass dissolution maintains the concentration of elements at a certain level, so the use of feldspar Na-K-geothermometers leads to erroneous estimates.

If crystalline feldspars, albite, anorthite and microcline are added to feldspar glass, the glass dissolves and recrystallizes into corresponding minerals, and Na-K-geothermometer eventually is close to Fournier equation. However, still during glass dissolution the  $C(\text{Na})/C(\text{K})$  ratio varies weakly, within 11-12.2 (for ppm) for a wide temperature range. Therefore, the presence of glass causes apparent warming of the geothermal reservoir and can lead to significant errors in temperature estimations.

*K-montmorillonite + Na-montmorillonite + Ca-montmorillonite + water system (TR\_T\_mont\_Ca\_#9).* K-montmorillonite (montmor-k), Na-montmorillonite (montmor-na), Ca-montmorillonite (montmor-ca) phases were taken as initial phases. The volume fractions of all three minerals were equal, and were 1/3. Simulation time was equal to 1000 years; at each simulation step local chemical water-rock equilibrium was assumed.

The Na/K ratio is poorly linearised in Arrhenius coordinates and varies in a small range – 1.5-6 (for ppm). A high value of the ratio is typical for low temperature and vice



*Mordenite + clinoptilolite (clinopt/10) + water (+/- heulandite) system (Mor\_Heu\_no\_Fels\_#9).* Mordenite (fraction 0.3), clinoptilolite (clinopt/10 fraction 0.3), and noncrystalline SiO<sub>2</sub> (fraction 0.4) were taken as initial phases. Opal was set in chemical equilibrium to thermal water; for zeolites the dissolution kinetic constant was set within the range 10<sup>-15</sup>-10<sup>-18</sup>, and the deposition kinetic constant took values from 10<sup>-19</sup>-10<sup>-20</sup>, activation energy was estimated to be 58 kJ/mol. The simulation time was equal to 1000 years.

Simulation results show that, under geothermal reservoir and alkaline conditions, clinoptilolite and heulandite precipitate at a high rate rapidly reaching saturation, while mordenite dissolves insignificantly. Therefore, in order to obtain the desired dependencies, the authors varied kinetic parameters such as deposition and dissolution rates for mordenite, heulandite and clinoptilolite. We found that the ratio of sodium and potassium concentrations was largely affected by the zeolite precipitation rate. It is important that the ratio of sodium and potassium concentrations vary between 13 and 20 (for ppm) within the temperature range of 25-250 °C. The linearisation of the ratios in Arrhenius coordinates is shown in the figure, which demonstrates two sections: a steeper high-temperature section and a flatter low-temperature section (Fig.7).

Zeolite geothermometer equations for high temperatures of 150-250 °C are as follows:

$$t = \frac{-349}{\lg \left[ \frac{C(\text{Na}^+)}{C(\text{K}^+)} \right] - 1.949} - 273.15 \text{ (for ppm);}$$

for temperatures of 25-150 °C geothermometer equations are as follows:

$$t = \frac{-12}{\lg \left[ \frac{C(\text{Na}^+)}{C(\text{K}^+)} \right] - 1.151} - 273.15 \text{ (for ppm).}$$

Note this low sodium-potassium ratio for waters that are in contact with zeolites, so the calculation using the feldspar equation results in inflated temperatures.

**Discussion.** The study of geyserite deposits from Geyser Velikan (Giant) shows the formation of amorphous zeolites in association with opal and quartz. Observation of the composition of the deposits shows a decrease in their crystallinity over the period of 2018-2021, which may be due to a certain decrease in the pH of the thermal solution. In general, the pH of the discharging solutions is high, alkaline (8-9), and favorable for zeolite formation. At the same time, the heated soils from the Valley of Geysers have a composition similar to that of heated soils from other thermal fields in Kamchatka and contain montmorillonite, which crystallizes in near-neutral and weakly acidic solutions. Such environment is formed when pore solutions of soils interact with air oxygen, resulting in

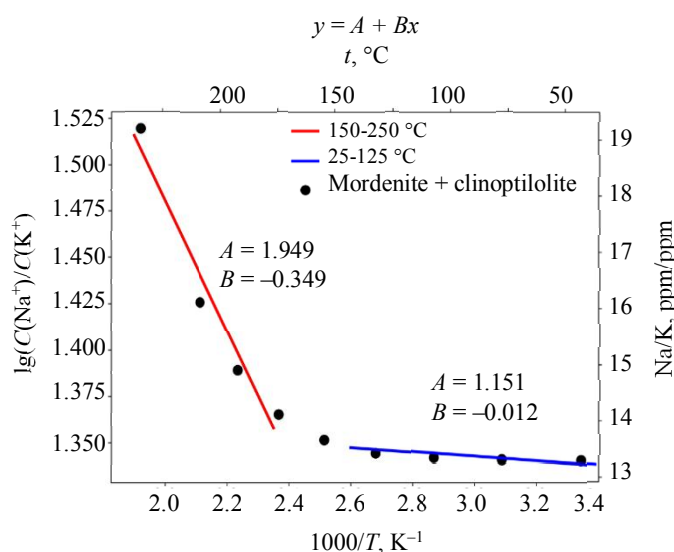


Fig. 7. Linear plots in Arrhenius coordinates for the sodium-potassium ratio in the function of temperature for mordenite and clinoptilolite



crystallization of skeleton salt deposits on the day surface, usually associated with layered silicates including montmorillonite.

Volcanic glass has a significant impact on geothermometer readings due to its good solubility compared to other minerals of associations. In alkaline environments, the solubility of silicate glasses increases by several orders of magnitude, hence the glass shows a significant impact on the Na/K ratio in natural reservoirs with alkaline solutions. Moreover, during glass dissolution the Na/K ratio, according to simulation results, is 11-12.2 in the temperature range of 25-250 °C, for the feldspar geothermometer it lies within 170-180 °C.

Smectite selectively absorbs sodium, and, according to the simulation results, the sodium/potassium ratio is reduced to a range of 1.5-6 in the temperature range 25-250 °C. The Na-K-geothermometer estimate of reservoir temperature for waters coming into equilibrium with smectite minerals gives inflated values, so the smectite impact on the Na-K-geothermometer is quite noticeable and is expressed in apparent warming of the reservoir. However, the application of the smectite geothermometer for determination of discharge temperatures in thermal fields, mud and mud and water pools, pore solutions of heated soils and steam and gas jets, provided montmorillonite is a dominating mineral, shows good agreement between estimated and measured temperatures during sampling. Therefore, the smectite geothermometer is useful in thermal fields, if the montmorillonite controls the sodium-potassium ratio.

Zeolites act similarly to montmorillonite, lowering the sodium-potassium ratio to a range of 13-19, within the temperature range of 25-250 °C, which according to the feldspar geothermometer corresponds to temperature range of 140-170 °C. The sensitivity of the geothermometer to temperature depends on the absolute value of parameter B: decrease in this parameter causes the decrease in the geothermometer sensitivity. Therefore, zeolite and volcanic glass based geothermometers are the least sensitive to temperature, then comes the montmorillonite geothermometer, which may have a limited application within thermal fields, while the feldspar geothermometer is the most sensitive.

Based on the results of the TOUGHREACT-simulation, we have derived Na-K-geothermometer equations for thermal solution equilibrium with feldspars, montmorillonite, zeolites and volcanic glass. Both categories of secondary minerals are capable of rapid cation exchange with contacting solutions, which can cause a failure in the feldspar Na-K-geothermometer readings. Consideration of the interaction between thermal waters and secondary minerals with ion-exchange properties has shown that zeolites and montmorillonite can affect feldspar geothermometer readings through controlling the sodium-potassium ratio in a solution. Minerals from these groups generally reduce the  $C(\text{Na}^+)/C(\text{K}^+)$  ratio resulting in inflated values for calculated reservoir temperatures. The failure of the Na-K-geothermometer due to contact with ion-exchange minerals is almost instantaneous, within a few tens of minutes, whereas the equilibrium with the feldspars is much slower, taking years or more to reach.

Volcanic glass in alkaline thermal solutions dissolves relatively quickly and thus is able to control the sodium-potassium ratio in the solution. Failures in the feldspar geothermometer readings caused by glass dissolution show an inflated temperature in the reservoir.

The feldspar geothermometer, based on simulation results, for the range of 25-200 °C:

$$t = \frac{1239}{\lg \left[ \frac{C(\text{Na}^+)}{C(\text{K}^+)} \right] + 1.683} - 273.15 \text{ (for ppm);}$$

within the range of 125-200 °C, the geothermometer equation based on volcano glass is as follows



$$t = \frac{8.5}{\lg \left[ \frac{C(\text{Na}^+)}{C(\text{K}^+)} \right] - 1.034} - 273.15 \text{ (for ppm),}$$

within the range of 25-125 °C,  $t = \frac{37}{\lg \left[ \frac{C(\text{Na}^+)}{C(\text{K}^+)} \right] - 0.961} - 273.15 \text{ (for ppm);}$

in the range of 25-150 °C, the equation for the smectite geothermometer is as follows

$$t = \frac{612}{\lg \left[ \frac{C(\text{Na}^+)}{C(\text{K}^+)} \right] + 1.267} - 273.15 \text{ (for ppm);}$$

zeolite geothermometer equations for high temperatures, 150-250 °C

$$t = \frac{-349}{\lg \left[ \frac{C(\text{Na}^+)}{C(\text{K}^+)} \right] - 1.949} - 273.15 \text{ (for ppm),}$$

for temperature range of 25-150 °C  $t = \frac{-12}{\lg \left[ \frac{C(\text{Na}^+)}{C(\text{K}^+)} \right] - 1.151} - 273.15 \text{ (for ppm).}$

History of changes in the chemical composition of geysers over the period of 1968-2020 shows the trend of decreasing chloride ion concentration [14, 46] which is explained by: decrease in deep heat transfer fluid inflow due to the decreasing trend of chloride ion concentration –1.1 ppm/year, from the initial concentration of 900 ppm, 1969-2003; additional dilution due to inflow of infiltration water from the Geyser River since catastrophic collapse in 2007 (lowering of chloride ion concentration to 780 ppm on average in Geyser Velikan).

If we use chloride ion as a zero valent tracer of geofiltration processes and assume chloride ion concentration in the parent fluid to be  $C_p = 810$  ppm as of 2002 [14], chloride ion concentration in the Geyser River  $C_r = 100$  ppm, with range from 43 to 167 ppm [59], the share of infiltration water in geyser discharge can be estimated as follows:

$$X = (C_p - C) / (C_p - C_r).$$

This ratio shows that the content of infiltration water (which is most probably “smectite water”) is estimated to be 5 %. If the chloride ion concentration in the parental fluid is taken as  $C_p = 900$  ppm [52], the estimated content of infiltration water increases to 15 %. Is it possible, based on the above, to combine two Na-K-geothermometers: deep feldspar and infiltration – smectite? Probably yes, but it requires a simulation with distributed parameters (not zero-dimensional), which simultaneously includes inflows of both the deep heat transfer fluid (parental fluid) and infiltration water. Such simulation is a task for yet further research.

**Conclusion.** Using TOUGHREACT-simulation on a one-element model (zero-dimensional) for hydrogeological conditions of the Geyser reservoir (the Valley of Geysers, Kamchatka), we reproduced previously known Na-K feldspar geothermometer [11, 25] and obtained new formulae for three Na-K-geothermometers: zeolite, smectite, and volcanic glass based. For practical purposes the use of the presented simulation and geothermometer equations contributes to the update for forecasting of catastrophic events as well as estimation of their geochemical consequences.





The authors have revealed that interaction between thermal water and volcanic glass causes Na/K-ratio varies within 11-12.2 (for ppm), for smectite this ratio lies within 1.5-6 (for ppm), for zeolites Na/K ratio lies within 13-19 (for ppm), within the temperature range 25-250 °C. The widest range is noted for feldspars, for which Na/K ratio lies within 6-300 (for ppm).

Over the period of 2010-2018, for geyser waters, the  $C(\text{Na}^+)/C(\text{K}^+)$  ratios lie in the range 5-15 (for ppm), the upper limit of the range corresponds to the feldspar geothermometer with temperatures of 160-180 °C and corresponds to the reservoir condition recorded before the mudslides. Values with a reduced sodium-potassium ratio are close to smectite waters, with temperatures within the range of 5-50 °C. The situation corresponds to the contact between waters that discharge to the surface in the form of geyser fountains and heated soils composed of smectite, at which the Na/K ratio decreases. It is likely that the smectite waters are responsible for mistakes in the feldspar geothermometer readings when we revealed obvious reservoir temperature values that exceeded the range of 160-180 °C.

The chemical timeline for chloride ion, which is considered as a zero valent tracer in the geofiltration processes, shows that a significant amount of infiltration water has been entering the Geyser reservoir after 2007, with the estimated mass fraction of 5-15 %. Most likely, this is “smectite water” formed as a result of chemical interaction between river water from the Geyser River and hydrothermally altered (smectite) rocks of the upper relative aquaclude (see Fig.3).

Thus, Na-K feldspar geothermometer readings [11, 25] up to 260-280 °C recorded in recent years (see Fig.1) may indicate the dilution effect caused by smectite waters. The application of thermohydrodynamic-chemical simulation with distributed parameters is necessary to estimate the true temperature in the Geyser reservoir, and this is the task for further research.

*The authors are grateful to N.B.Zhuravlev, a Junior Researcher at the Laboratory of Heat and Mass Transfer at the Institute of Volcanology and Seismology of the FEB RAS, for his help in the field study and discussion of the material, and to P.I.Shpilenok, D.M.Panicheva, and E.L.Subbotina, the staff of Kronotsky State Nature Biosphere Reserve for help in preparing and conducting field work in the Valley of Geysers and Uzon Caldera.*

## REFERENCES

1. Bondareva G.L. Estimation of temperature conditions of mineral water formation in the Pyatigorsk deposit. *Razvedka i okhrana nedr.* 2011. N 3, p. 40-42 (in Russian).
2. Lavrushin V.Y., Guliev I.S., Kikvadze O.E. et al. Waters from Mud Volcanoes of Azerbaijan: Isotopic-Geochemical Properties and Generation Environments. *Lithology and Mineral Resources.* 2015. Vol. 50. N 1, p. 1-25 (in Russian). DOI: [10.7868/S0024497X15010036](https://doi.org/10.7868/S0024497X15010036)
3. Chelnokov G.A., Bragin I.V., Kharitonova N.A. et al. Geochemistry and formation conditions of the Ul'sk thermal spring, the Okhotsk Sea coast, Khabarovsk Territory. *Tikhookeanskaya geologiya.* 2019. Vol. 38. N 2, p. 73-85 (in Russian). DOI: [10.30911/0207-4028-2019-38-2-73-85](https://doi.org/10.30911/0207-4028-2019-38-2-73-85)
4. Chelnokov G.A., Lavrushin V.Yu., Aidarkozhina A.S. et al. New data on gas composition and geothermometry of mineral waters of Kyrgyzstan. Water-rock interaction: geological evolution proceedings of the fourth all-Russian scientific conference with international participation. Ulan-Ude: Buryatskiy nauchnyy tsentr SO RAN, 2020, p. 111-113 (in Russian). DOI: [10.31554/978-5-7925-0584-1-2020-111-113](https://doi.org/10.31554/978-5-7925-0584-1-2020-111-113)
5. Kireeva T.A., Salikhov F.S., Bychkov A.Yu., Kharitonova N.A. New Data on Microelement and Isotope Composition of Thermal Springs in Tajikistan. Water-rock interaction: geological evolution Proceedings of The Third all-Russian Scientific Conference With International Participation. Ulan-Ude: Buryatskiy nauchnyy tsentr SO RAN, 2018, p. 292-295 (in Russian). DOI: [10.31554/978-5-7925-0536-0-2018-292-295](https://doi.org/10.31554/978-5-7925-0536-0-2018-292-295)
6. Kireeva T.A., Salikhov F.S., Bychkov A.Yu., Kharitonova N.A. Chemical composition of waters and conditions of formation of some thermal springs in Tadzhikistan. *Geokhimiya.* 2020. Vol. 65. N 4, p. 379-391 (in Russian). DOI: [10.31857/S0016752520030061](https://doi.org/10.31857/S0016752520030061)
7. Badminov P.S., Ivanov A.V., Pisarskii B.I., Orgilyanov A.I. Okinskaya hydrothermal system (Eastern Sayan). *Vulkanologiya i seismologiya.* 2013. N 4, p. 27-39 (in Russian). DOI: [10.7868/S0203030613040020](https://doi.org/10.7868/S0203030613040020)
8. Zippa E.V., Guseva N.V., Sun Zh., Chen G. Estimation of Circulation Temperatures of Thermal Waters in Jiangxi Province Using Different Geothermometers. *Earth Sciences.* 2019. N 10, p. 52-57 (in Russian). DOI: [10.17513/issue.37213](https://doi.org/10.17513/issue.37213)
9. Chelnokov G.A., Bragin I.V., Kharitonova N.A. New isotope-geochemical data on Tavatum thermal waters (Magadanskaya Oblast). *Tikhookeanskaya geologiya.* 2021. Vol. 40. N 5, p. 104-114 (in Russian). DOI: [10.30911/0207-4028-2021-40-5-104-114](https://doi.org/10.30911/0207-4028-2021-40-5-104-114)
10. Alekseev V.A. Kinetics and mechanisms of feldspar reactions with aqueous solutions. Moscow: GEOS, 2002, p. 246 (in Russian).



11. Truesdell A.H., Jones B.F. WATEQ, a computer program for calculating chemical equilibria of natural waters. *Journal of Research of the U.S. Geological Survey*. 1974. Vol. 2. N 2, p. 233-248.
12. Fournier R.O., Potter II R.W. Magnesium correction to the Na-K-Ca chemical geothermometer. *Geochimica et Cosmochimica Acta*. 1979. Vol. 43. Iss. 9, p. 1543-1550. DOI: [10.1016/0016-7037\(79\)90147-9](https://doi.org/10.1016/0016-7037(79)90147-9)
13. Frolova Yu.V., Gvozdeva I.P., Chernov M.S., Kuznetsov N.P. Engineering and geological aspects of hydrothermal transformations of tuffogenic rocks of the Valley of Geysers (the Kamchatka Peninsula). *Inzhenernaya geologiya*. 2015. N 6, p. 30-42 (in Russian).
14. Kiryukhin A.V. Geothermofluidomechanics hydrothermal, volcanic and hydrocarbon system. St. Petersburg: Eco-Vector IP, 2020, p. 431 (in Russian).
15. Kiryukhin A., Sugrobov V., Sonnenthal E. Geysers Valley CO<sub>2</sub> Cycling Geological Engine (Kamchatka, Russia). *Geofluids*. 2018. Vol. 2018. N 1963618, p. 1-16. DOI: [10.1155/2018/1963618](https://doi.org/10.1155/2018/1963618)
16. Spycher N., Peiffer L., Sonnenthal E.L. et al. Integrated multicomponent solute geothermometry. *Geothermics*. 2014. Vol. 51, p. 113-123. DOI: [10.1016/j.geothermics.2013.10.012](https://doi.org/10.1016/j.geothermics.2013.10.012)
17. Kugaenko Y.A., Saltykov V.A., Gorbatiykov A.V., Stepanova M.Y. The Model of the Uzon-Geizernaya Volcano-Tectonic Depression and Kikhpinych Volcano, Kamchatka, from the Joint Analysis of Microseismic Sounding Data and Local Geodynamic Activity. *Izvestiya, Physics of the Solid Earth*. 2015. Vol. 51. N 3, p. 403-418. DOI: [10.7868/S0002333715030096](https://doi.org/10.7868/S0002333715030096)
18. Kiryukhin A. V., Rychkova T.V., Sergeeva A.V. Modeling of the Conditions for the Formation of Permeable Geyser Channels in Acid Volcanism Areas. *Journal of Volcanology and Seismology*. 2020. N 2, p. 3-16 (in Russian). DOI: [10.31857/S0203030620020030](https://doi.org/10.31857/S0203030620020030)
19. Sergeeva A., Kiryukhin A. Secondary minerals in the geysers of the Geysers Valley (Kamchatka). *E3S Web of Conferences*. 2019. Vol. 98. N 08019, p. 1-5. DOI: [10.1051/e3sconf/20199808019](https://doi.org/10.1051/e3sconf/20199808019)
20. Sergeeva A.V., Denisov D.K., Nazarova M.A. Clay mineral assemblages in recent thermal anomalies of Southern Kamchatka. *Russian Geology and Geophysics*. 2019. Vol. 60. N 11, p. 1267-1277. DOI: [10.15372/RGG2019090](https://doi.org/10.15372/RGG2019090)
21. Semenov I.N., Klink G.V., Lebedeva M.P. et al. The variability of soils and vegetation of hydrothermal fields in the Valley of Geysers at Kamchatka Peninsula. *Scientific Reports*. 2021. Vol. 11. Iss. 1. N 11077. DOI: [10.1038/s41598-021-90712-7](https://doi.org/10.1038/s41598-021-90712-7)
22. Sudarikov S.M. Modeling of geochemical processes in the submarine discharge zone of hydrothermal solutions. *Journal of Mining Institute*. 2017. Vol. 225, p. 284-291. DOI: [10.18454/PMI.2017.3.284](https://doi.org/10.18454/PMI.2017.3.284)
23. Sudarikov S., Petrov V., Narkevsky E. et al. In-Situ Study Methods Used in the Discovery of Sites of Modern Hydrothermal Ore Formation on the Mid-Atlantic Ridge. *Minerals*. 2022. Vol. 12. Iss. 10. N 1219. DOI: [10.3390/min12101219](https://doi.org/10.3390/min12101219)
24. Sergeeva A.V., Zhitova E.S., Nuzhdaev A.A., Nazarova M.A. Modeling the Mineral Formation Process on Thermoanomalies with Ammonium-Sulfate Thermal Waters: the Role of Acidity (pH). *Journal of Volcanology and Seismology*. 2022. N 1, p. 39-53 (in Russian). DOI: [10.31857/S0203030621060092](https://doi.org/10.31857/S0203030621060092)
25. Truesdell A.H., Fournier R.O. Calculation of Deep Temperatures in Geothermal Systems from the Chemistry of Boiling Spring Waters of Mixed Origin. Second United Nations Symposium on the Development and Use of Geothermal Resources, San Francisco, May, 1975. Vol. 1, p. 837-844.
26. Tamuna B., Khamizov R.Kh., Bavizhev M.D., Konov M.A. The effect of microwave treatment of clinoptilolite on its ion-exchange kinetic properties. *Sorbtionnyye i khromatograficheskie protsessy*. 2016. Vol. 16. N 6, p. 803-812 (in Russian).
27. Kolesnikova L.G., Lankin S.V., Yurkov V.V. Ionic transfer in clinoptilolite. Blagoveshchensk: Izd-vo Blagoveshchenskogo gosudarstvennogo pedagogicheskogo universiteta, 2007, p. 113 (in Russian).
28. Kolesnikova L.G. Ionic exchange in zeolites. *Problemy ekologii Verkhnego Priamurya*. 2012. Vol. 14, p. 12-45 (in Russian).
29. Kolesnikova L.G., Filippova T.S., Klyuchevskaya T.G. Composition and thermodynamic parameters of the ionic exchange of zeolites from the Vanginskoye deposit in the Amur Region. *Problemy ekologii Verkhnego Priamurya*. 2009. Vol. 11, p. 23-41 (in Russian).
30. Shkurenko G.Yu. Ion-exchange properties of natural geylandite: Avtoref. dis. ... kand. khim. nauk. Kemerovo: Kemerovskii gosudarstvennyi universitet, 2004, p. 16 (in Russian).
31. Bobonich F.M., Patrylak K.I., Levchuk M.M. et al. Influence of chemical modification on catalytic properties of clinoptilolite and mordenite in *n*-hexane hydroisomerization. *Catalysis and Petrochemistry*. 2001. N 9-10, p. 98-102 (in Russian).
32. Razmahnin K.K., Milyutin V.V., Khatkova A.N. Geo-Ecological Aspects of Natural Zeolites Using. *Interexpo GEO-Siberia*. 2019. Vol. 2. N 4, p. 246-255 (in Russian). DOI: [10.33764/2618-981X-2019-2-4-246-255](https://doi.org/10.33764/2618-981X-2019-2-4-246-255)
33. Khatkova A.N. Perspectives of using zeolites to improve industrial and environmental safety at industrial facilities in Russia. Kulaginskii chteniya: tekhnika i tekhnologii proizvodstvennykh protsessov: Materialy XX Mezhdunarodnoi nauchno-prakticheskoi konferentsii. Chita: Zabaikalskii gosudarstvennyi universitet, 2020. Part I, p. 7-15 (in Russian).
34. Vezentsev A.I., Dobrodomova E.V., Peristaya L.F. et al. Mineralogical composition of clay of Sergievskiy deposit as a sorbent of heavy metal ions from aqueous solutions. *Voda: khimiya i ekologiya*. 2012. N 10 (52), p. 78-84 (in Russian).
35. Sarapulova G.I. Geochemical approach in assessing the technogenic impact on soils. *Journal of Mining Institute*. 2020. Vol. 243, p. 388-392. DOI: [10.31897/PMI.2020.3.388](https://doi.org/10.31897/PMI.2020.3.388)
36. Erzova V.A., Rumynin V.G., Nikulenkov A.M. et al. Forecast of radionuclide migration in groundwater of the zone affected by construction drainage at the Leningrad NPP-2. *Journal of Mining Institute*. 2023. Vol. 260, p. 194-211. DOI: [10.31897/PMI.2022.27](https://doi.org/10.31897/PMI.2022.27)
37. Dashko R.E., Lokmatikov G.A. Comprehensive safety assessment of radioactive waste disposal in clayey formations (case study of St. Petersburg region). *Mining Informational and Analytical Bulletin*. 2022. Iss. 10-1, p. 66-76. DOI: [10.25018/0236\\_1493\\_2022\\_101\\_0\\_66](https://doi.org/10.25018/0236_1493_2022_101_0_66)
38. Palyanitsina A.N., Sukhikh A.S. Peculiarities of assessing the reservoir properties of clayish reservoirs depending on the water of reservoir pressure maintenance system properties. *Journal of Applied Engineering Science*. 2020. Vol. 18. Iss. 1, p. 10-14. DOI: [10.5937/jaes18-24544](https://doi.org/10.5937/jaes18-24544)



39. Pashkevich M.A., Bykova M.V. Improvability of measurement accuracy in determining the level of soil contamination with petroleum products. *Mining Informational and Analytical Bulletin*. 2022. N 4, p. 67-86 (in Russian). DOI: [10.25018/0236\\_1493\\_2022\\_4\\_0\\_67](https://doi.org/10.25018/0236_1493_2022_4_0_67)
40. Mustafaev A.S., Popova A.N., Sukhomlinov V.S. A New Technique of Eliminating the Actual Plasma Background When Calibrating Emission Spectrometers with a CCD Recording System. *Applied Sciences*. 2022. Vol. 12. Iss. 6. N 2896. DOI: [10.3390/app12062896](https://doi.org/10.3390/app12062896)
41. Popova A.N., Sukhomlinov V.S., Mustafaev A.S. A New Intensity Adjustment Technique of Emission Spectral Analysis When Measured at the Upper Limit of the Dynamic Range of Charge-Coupled Devices. *Applied Sciences*. 2022. Vol. 12. Iss. 13. N 6575. DOI: [10.3390/app12136575](https://doi.org/10.3390/app12136575)
42. El-Batouti M., Sadek O.M., Assaad F.F. Kinetics and thermodynamics studies of copper exchange on Na-montmorillonite clay mineral. *Journal of Colloid and Interface Science*. 2003. Vol. 259. N 2, p. 223-227. DOI: [10.1016/S0021-9797\(02\)00173-X](https://doi.org/10.1016/S0021-9797(02)00173-X)
43. Inoue A., Minato H. Ca-K Exchange Reaction and Interstratification in Montmorillonite. *Clays and Clay Minerals*. 1979. Vol. 27. Iss. 6, p. 393-401. DOI: [10.1346/CCMN.1979.0270601](https://doi.org/10.1346/CCMN.1979.0270601)
44. Fletcher P., Sposito G. The chemical modelling of clay/electrolyte interactions for montmorillonite. *Clay Minerals*. 1989. Vol. 24. N 2, p. 375-391. DOI: [10.1180/claymin.1989.024.2.14](https://doi.org/10.1180/claymin.1989.024.2.14)
45. Shainberg I., Alperovitch N.I., Keren R. Charge Density and Na-K-Ca Exchange on Smectites. *Clays and Clay Minerals*. 1987. Vol. 35. Iss. 1, p. 68-73. DOI: [10.1346/CCMN.1987.0350109](https://doi.org/10.1346/CCMN.1987.0350109)
46. Tournassat C., Bizi M., Braibant G., Crouzet C. Influence of montmorillonite tactoid size on Na-Ca cation exchange reactions. *Journal of Colloid and Interface Science*. 2011. Vol. 364. Iss. 2, p. 443-454. DOI: [10.1016/j.jcis.2011.07.039](https://doi.org/10.1016/j.jcis.2011.07.039)
47. Di Xu, Xiang Zhou, Xiangke Wang. Adsorption and desorption of Ni<sup>2+</sup> on Na-montmorillonite: Effect of pH, ionic strength, fulvic acid, humic acid and addition sequences. *Applied Clay Science*. 2008. Vol. 39. Iss. 3-4, p. 133-141. DOI: [10.1016/j.clay.2007.05.006](https://doi.org/10.1016/j.clay.2007.05.006)
48. Taran Yu.A., Ryabinin G.V., Pokrovski B.G. et al. Mineral Waters of the Avachinsky Depression, Kamchatka. *Bulletin of Kamchatka Regional Association "Educational-Scientific Center"*. *Earth Sciences*. 2021. Iss. 50. N 2, p. 22-39 (in Russian). DOI: [10.31431/1816-5524-2021-2-50-22-39](https://doi.org/10.31431/1816-5524-2021-2-50-22-39)
49. Kiryukhin A.V., Rychkova T.V., Dubrovskaya I.K. Hydrothermal system in Geysers Valley (Kamchatka) and triggers of the Giant landslide. *Applied Geochemistry*. 2012. Vol. 27, p. 1753-1766.
50. Belousov V.I., Grib E.N., Leonov V.L. Geological positions of hydrothermal systems of the Valley of Geysers and Uzon Caldera. *Journal of Volcanology and Seismology*. 1983. N 1, p. 65-79 (in Russian).
51. Kalinin D.F., Egorov A.S., Bolshakova N.V. Oil and Gas Potential of the West Kamchatka Coast and Its Relation to the Structural and Tectonic Structure of the Sea Of Okhotsk Region Based on Geophysical Data. *Bulletin of Kamchatka Regional Association "Educational-Scientific Center"*. *Earth Sciences*. 2022. Iss. 53. N 1, p. 59-75 (in Russian). DOI: [10.31431/1816-5524-2022-1-53-59-75](https://doi.org/10.31431/1816-5524-2022-1-53-59-75)
52. Belousov V.I., Sugrobov V.M. Geological and hydrogeothermal conditions of geothermal areas and hydrothermal systems of Kamchatka. *Gidrotermalnye sistemy i termalnye polya Kamchatki*. Vladivostok: Izd-vo Dalnevostochnogo nauchnogo tsentra AN SSSR, 1976, p. 5-22 (in Russian).
53. Tianfu Xu, Sonnenthal E., Spycher N., Pruess K. TOUGHREACT – A simulation program for non-isothermal multiphase reactive geochemical transport in variably saturated geologic media: Applications to geothermal injectivity and CO<sub>2</sub> geological sequestration. *Computers & Geosciences*. 2006. Vol. 32. Iss. 2, p. 145-165. DOI: [10.1016/j.cageo.2005.06.014](https://doi.org/10.1016/j.cageo.2005.06.014)
54. Shulyupin A.N. Flow instability in producing well at flash-steam fields. *Journal of Mining Institute*. 2016. Vol. 220, p. 551-555. DOI: [10.18454/PMI.2016.4.551](https://doi.org/10.18454/PMI.2016.4.551)
55. Sergeeva A.A., Kiryukhin A.V., Usacheva O.O. et al. Influence of Secondary Minerals on Na-K Geothermometer Readings in the Valley of Geysers Hydrothermal System (Kronotsky Nature Reserve, Kamchatka). *Geothermal Volcanology Workshop*. Petropavlovsk-Kamchatsky: Institute of Volcanology and Seismology FEB RAS, 2022, p. 90-94 (in Russian).
56. Fournier R.O. Application of water geochemistry to geothermal exploration and reservoir engineering. *Geothermal Systems. Principle and Case Histories*. Hoboken: John Wiley & Sons, 1981, p. 109-143.
57. Fournier R.O., Truesdell A.H. Chemical indicators of subsurface temperature applied to hot spring waters of Yellowstone National Park, Wyoming, U.S.A. *Geothermics*. 1970. Vol. 2. Part 1, p. 529-535. DOI: [10.1016/0375-6505\(70\)90051-9](https://doi.org/10.1016/0375-6505(70)90051-9)
58. Kalacheva E.G., Rychagov S.N., Nuzhdaev A.A., Koroleva G.P. The Geochemistry of Steam Hydrothermal Occurrences in the Koshelev Volcanic Massif, Southern Kamchatka. *Journal of Volcanology and Seismology*. 2016. Vol. 10. N 3, p. 188-202. DOI: [10.7868/S0203030616030044](https://doi.org/10.7868/S0203030616030044)
59. Kiryukhin A.V., Polyakov A.Y., Zhuravlev N.B. et al. Dynamics of natural discharge of the hydrothermal system and geyser eruption regime in the Valley of Geysers, Kamchatka. *Applied Geochemistry*. 2022. Vol. 136. N 105166. DOI: [10.1016/j.apgeochem.2021.105166](https://doi.org/10.1016/j.apgeochem.2021.105166)

**Authors:** Anastasia V. Sergeeva, Candidate of Chemistry Sciences, Senior Researcher, [anastavalers@gmail.com](mailto:anastavalers@gmail.com), <https://orcid.org/0000-0001-5127-347X> (Institute of Volcanology and Seismology FEB RAS, Petropavlovsk-Kamchatsky, Russia), Alexey V. Kiryukhin, Doctor of Geological and Mineralogical Sciences, Chief Researcher, Senior Researcher, <https://orcid.org/0000-0001-5468-1452> (Institute of Volcanology and Seismology FEB RAS, Petropavlovsk-Kamchatsky, Russia; Kronotsky State Nature Biosphere Reserve, Yelizovo, Russia), Olga O. Usacheva, Junior Researcher, <https://orcid.org/0000-0002-0781-3448> (Institute of Volcanology and Seismology FEB RAS, Petropavlovsk-Kamchatsky, Russia), **Tatiana V. Rychkova**, Candidate of Geological and Mineralogical Sciences, Senior Researcher, <https://orcid.org/0000-0002-6844-8771> (Institute of Volcanology and Seismology FEB RAS, Petropavlovsk-Kamchatsky, Russia), Elena V. Kartasheva, Head of the Analytical Center, <https://orcid.org/0000-0002-0518-7412> (Institute of Volcanology and Seismology FEB RAS, Petropavlovsk-Kamchatsky, Russia), Mariya A. Nazarova, Junior Researcher, <https://orcid.org/0000-0001-6839-6599> (Institute of Volcanology and Seismology FEB RAS, Petropavlovsk-Kamchatsky, Russia), Anna A. Kuzmina, Junior Researcher, <https://orcid.org/0000-0002-1428-6447> (Institute of Volcanology and Seismology FEB RAS, Petropavlovsk-Kamchatsky, Russia).

The authors declare no conflict of interests.